Dynamic Economic Dispatch and Transient Control of Distributed Generators in a Microgrid

Jameel Ahmad, Muhammad Tahir, *Member, IEEE*, and Sudip K. Mazumder, *Fellow, IEEE*

***Abstract*—Microgrids have multiple distributed generators (DGs) with increased penetration of renewable energy sources. Efficient integration of these DGs in a microgrid, whether in grid-connected or islanded mode, poses many challenges, such as optimal power sharing, control of load-side and generator-side transients, and economic dispatch (ED), to name a few. Different control strategies for power sharing and ED fall short in providing good dynamic performance. To address this issue, we propose a novel solution that provides ED with improved dynamic performance. Specifically, the ED problem employs dynamic performance controller based on proportional–integral–derivative control for improved performance by using an augmented Lagrangian-based approach. For the distributed coordinated control of DGs, we utilize a multiagent system architecture. The performance evaluation results show that the proposed solution for ED improves the overall system performance of the microgrid. The system achieves an optimal state, where DGs operate at minimum cost while improving the transient response during load or generator switching.**

***Index Terms*—Distributed generation, dynamic performance, islanded microgrid, multiagent system (MAS), optimized control.**

NOMENCLATURE

w	Operating frequency in rad/s.
w_o	Nominal frequency.
E	Operating voltage.
E_o	Nominal system voltage.
$\alpha_i, \beta_i, \gamma_i$	Generator cost coefficients.
a_i, b_i, c_i	Pollutant emission cost coefficients.
C	Generator cost function.
E_i	Emission cost function of ith generator.
k_p, k_i, k_d	PID controller gains.
z	Power variable.
L	Lagrangian function.
L_a	Augmented Lagrangian function.
M	Laplacian matrix.
p_{pv}	PV power.
L_d	Load demand.
u_i	Control law.
$f_r(p_{pv})$	Reliability cost of PV power.

Manuscript received July 1, 2017; revised April 10, 2018 and June 11, 2018; accepted July 19, 2018. Date of publication August 17, 2018; date of current version February 22, 2019. *(Corresponding author: Jameel Ahmad.)*

J. Ahmad is with the Department of Electrical Engineering, University of Management and Technology, Lahore, Lahore 54700, Pakistan, and also with the Department of Electrical Engineering, University of Engineering and Technology, Lahore, Lahore 54890, Pakistan (e-mail: jameel.ahmad@umt.edu.pk).

M. Tahir is with the Department of Electrical Engineering and Al-Khwarizmi Institute of Computer Science, University of Engineering and Technology, Lahore, Lahore 54890, Pakistan (e-mail: mtahir@uet.edu.pk).

S. K. Mazumder is with the Department of Electrical and Computer Engineering, University of Illinois at Chicago, Chicago, IL 60607 USA (e-mail: mazumder@ece.uic.edu).

Digital Object Identifier 10.1109/JSYST.2018.2859755

I. INTRODUCTION

AN ARBITRARY microgrid is a cluster of multiple distributed power sources. Distributed generation is the term often used for small-scale power generation, in which multiple distributed generators (DGs), usually of few megawatt (MW) [1], are connected to form a microgrid. The increased penetration and integration of microgrids in energy sector in recent years has raised many challenging problems, such as economic dispatch (ED), efficient control of power sources and timely communication of system variables, power quality concerns, load transients, and system harmonics. Due to limitations of conventional power sources and increased environmental concerns because of gaseous emissions, renewable energy sources along with storage system for backup are also becoming integral part of these microgrids. A microgrid meets energy needs of a small locality or injects excess power to the main utility grid. It can work either in an islanded or grid-connected mode. A microgrid should seamlessly switch between these two modes during its operation providing efficient control and power management. Islanding may occur due to unplanned disturbances or preplanned scheduling. While a disturbance may override the system for some time, transients are generated due to load switching [2]. In this study, an islanded mode of the microgrid operation is considered and the process of entering or leaving of a DG leads to transients in the microgrid. The coexistence of renewable sources in the microgrid makes the magnitude of these transients even more pronounced.

One of the key performance attributes of a microgrid is the ED, which is the process of determining the optimal operation of DGs to minimize the generation cost while meeting the load demands as well as operational constraints. Different solutions have been proposed for ED, which are broadly termed as dynamic ED (DED) and real-time ED. The DED problem is formulated as a two-stage primal-dual problem using Lagrangian relaxation [3]. The implementation of DED can be realized using either a centralized or a distributed control. In case of the centralized DED, all the DGs are controlled from a central control center [4], [5]. On the other hand, a distributed DED can be implemented by using a multiagent system (MAS) architecture

[6]–[8]. Cherukuri and Corts [6] have proposed a relaxation of ED (RED) problem using a distributed Laplacian-based first-order dynamics, which provides exponential convergence. The solution approach in [6] uses a non-smooth penalty function based approach to map the RED problem as an unconstrained optimization problem and performs a distributed allocation of loads to the set of DGs. The solution approach in [7] offers a distributed consensus control for optimized management of distributed generation resources for an islanded mode of the microgrid operation. The above-mentioned solution approaches suffer from the limited dynamic performance of economic dispatch.

Microgrid employs a hierarchical control strategy for its operation. At the bottom of the hierarchy is the primary control that maintains the operating voltage and frequency. The secondary control is responsible for active and reactive power controls, which is also termed as automatic generation control (AGC). To minimize the generation cost while meeting the load demands, we need to operate different DGs at the optimal power generation point. For that purpose, tertiary control is used to implement economic dispatch.

Conventionally, the ED problem is performed on a slower time scale. Although the conventional approaches to solve ED problem have been efficacious for traditional power systems, they fall short for a microgrid system with frequent transients and larger power fluctuations. This can be attributed to the fact that the load demand uncertainties as well as the number of renewable resources are on the rise. As a result, the generation system is exposed to large power fluctuations [9], resulting in frequent transients. Cost-based droop schemes for economic dispatch in islanded microgrids are presented in [10]. A robust two-stage approximate optimization approach is presented to schedule the energy generation under uncertainties to minimize long-term average operating cost in [11]. The first stage of optimization determines hourly unit commitment of the conventional generators (CGs) via a day-ahead scheduling, and the second stage performs economic dispatch of the CGs, energy storage systems, and energy trading via a real-time scheduling. Though the solution handles the uncertainties due to renewable generation and load demands, however, it offers an approximate optimization solution for the long-term operational cost. Peak-aware online economic dispatching for microgrids is studied in [12] considering competitive online algorithms that do not rely on prediction of the future input. System dynamics or transients, however, have not been considered in this paper. The focus was only on cost reduction. A two-stage control framework and a hybrid control method are proposed for active power real-time dispatch in islanded ac microgrids in [13]. However, the proposed solution suffers from slow dynamic response. The primal-dual algorithm based distributed ED solution also suffers from poor dynamic performance due to the presence of inherent integral controller as will be explained in Section III-A. In addition, the time gap between slower ED and faster AGC leads to reduced economical efficiency of the microgrid. Few studies have proposed to bridge this gap between ED and AGC. Integrating AGC and ED for real-time optimization is proposed in [14] and ED in the feedback loop is activated at discrete time instants that continuously sets the generator's set points. This is a suboptimal solution because AGC depends on ED, which is slower, while load keeps on changing on a faster time scale. The above-mentioned limitations demand for new solution approaches to the ED problem, which can respond to fast fluctuations in the generation as well as load.

To address this issue, the conventional primal-dual algorithm based ED is extended in this paper. Specifically, to achieve improved dynamic response, an augmented Lagrangian based dynamic control is proposed. The augmentation to the Lagrangian function allows us to implement a proportional–integral–derivative (PID) controller. In addition, for distributed control implementation, a multiagent-based system architecture is proposed. Traditionally, a multiagent-based architecture converges to the average consensus [15], which in case of distributed generation can provide equal load sharing or equivalently consensus among the DGs. This is a useful attribute for controlling DGs of equal rating. On the other hand, real-time ED can always require unequal load sharing among the DGs. To achieve any desired level of tradeoff between ED and generation consensus among DGs, a relaxation of consensus constraint is introduced. The proposed solution approach is equally useful for grid connected as well as islanded modes of operation. However, it is more effective for an islanded mode of operation, in which case transients can be more pronounced. Normally, ED problem and dynamic response problem are addressed separately in the literature. One key contribution of this paper is to embed dynamic response in ED optimization. In addition, some other contributions of this paper are as follows:

1) A fully distributed augmented Lagrangian-based PID control algorithm that can be applied to an islanded microgrid to improve the dynamic performance during transients;
2) Optimal power sharing of the generators;
3) Problem formulation for an economic-emission dispatch with PV-integrated transient control with distributed loads, such as electric vehicles (EVs).

This paper is organized as follows. In Section II-A, a microgrid system architecture with multiple generation systems is outlined. Details of the distributed control with the multiagent architecture is presented in Section II-B. The ED based on the conventional and proposed PID control along with emission reductions and integration of renewable energy resources is given in Section III. Performance evaluation results are provided in Section IV and this paper is concluded in Section V.

II. System Model

A. Microgrid System Architecture

Microgrids are classified based on their architectures, control, and communication interfaces as residential, industrial, or military microgrids. Our proposed microgrid system architecture is shown in Fig. 1 consisting of a mix of DGs of different types. In this model, renewable and nonrenewable energy sources are combined together in the form of a hybrid microgrid. DC–DC converters, dc–ac inverters, power management system, and controllable loads are some other system components

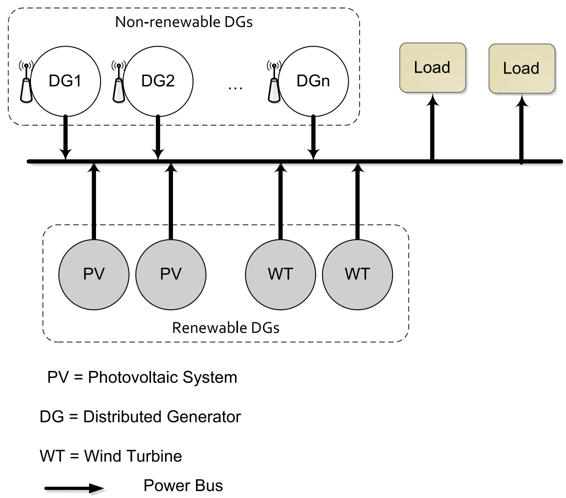

Fig. 1. Microgrid system architecture.

in a typical microgrid. Nonrenewable sources usually consist of conventional thermal generators, whereas major renewable energy sources include photovoltaic (PV) and wind-based systems. The presence of renewable energy sources also leads to disturbances in the form of power transients. Since our proposed microgrid is responsible for providing power to few MW loads, these transients cannot be neglected. The conventional thermal units have tight control of voltage and frequency specially when it is dictated by utility grid. When in islanded mode, the microgrid experiences transients due to fluctuations in load as well as renewable energy sources, and as a result, system dynamics are disturbed. In such a scenario, it becomes even more desirable to use control techniques that can provide improved dynamic performance.

As discussed in Section I, a three-layer hierarchical control is used in microgrids. Primary control maintains the operating voltage and frequency, whereas secondary control is responsible for active and reactive power controls, as shown in Fig. 2. Droop control and its variants for secondary control are provided in [16]–[18] and references therein. However, it is well known that poor load sharing and inferior dynamic performance are the key limitations of the droop control. Our proposed solution addresses these limitations by devising a multiagent structure for communication among the DGs and PID-based controller for improved dynamic performance for ED.

The ED problem is solved at tertiary control level and is responsible for dynamically updating $P_{\rm ref}$ and $Q_{\rm ref}$ set point values, which act as reference for secondary control as can be observed from Fig. 2. The multiagent structure helps in implementing ED at run time by continuously monitoring the system state of all DGs and provide this information to ED control (EDC). The cost optimization dynamics of EDC can be controlled by PID resulting in improved dynamic performance, which in turn results in better power sharing and control of transients. The presence of phase-locked loop (PLL), as observed from Fig. 2, is responsible to set reference frequency for a microgrid, when synchronized with the main grid. Since the proposed solution is at tertiary control level, secondary control for voltage

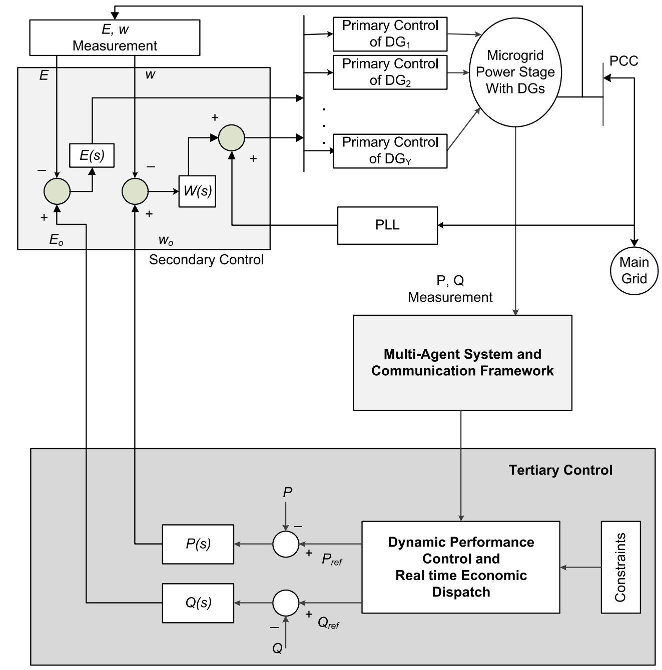

Fig. 2. Microgrid hierarchical control.

and frequency stabilizations is not the focus of this paper. Rather, it is anticipated that voltage and frequency controls are in place and are fully functional. Reader is referred to [16], [19] for more details on primary and secondary control loops.

B. Multiagent Communication Framework for Microgrid

To implement the above microgrid architecture, we consider a collection of Y DGs and define the corresponding set $\mathcal{Y} = \{1, 2, \ldots, Y\}$. Each DG_i has an associated set of neighboring DGs denoted by $Y_i \subset \mathcal{Y}$. The set Y_i includes all DGs that can communicate with DG_m and we assume that underlying communication link is bidirectional. This scenario can be modeled using an undirected graph $G = \{Y, E\}$, where E is the set of communication links among the communicating pairs of DGs. For graph G, we define a $Y \times Y$ adjacency matrix $A = A(G)$. Each entry $a_{i,m} \in A$ is set to 1, if we have $(i, m) \in E$, i.e., the corresponding communication link between DG_i and DG_m exists and to 0 otherwise. If $a_{i,m} = 1$, then we call DG_i and DG_m to be adjacent. From the communication perspective, degree d_i of a DG_i is defined as the number of adjacent DGs to it and is given by $d_i = \sum_{m \in Y_i, m \neq i} a_{i,m}$, $\forall i$. Let $D \in R^{Y \times Y}$ is the diagonal matrix with entries $d_i, i \in \{1, 2, \ldots, Y\}$, and is called degree matrix of graph G. Now, we can define graph Laplacian matrix as $M = D - A$. The matrix M has all row sums equal to zero, i.e., $M\mathbf{1} = 0$, where $\mathbf{1}$ is vector of all ones.

III. Optimized Control and ED

In the conventional ED, a constrained optimization problem is formulated and is solved by using the Lagrangian algorithm. As we will observe later, this approach is equivalent to an integral control and results in poor dynamic performance. To improve dynamic performance, an augmented Lagrangian based PID controller for ED will be proposed.

A. Conventional ED

The ED optimization problem with a quadratic cost function C_i is defined as

$$\sum_i C_i(z_i) = \sum_i \alpha_i z_i^2 + \beta_i z_i + \gamma_i \quad \forall i. \tag{1}$$

In (1), $z_i \in \mathbf{z}, \mathbf{z} \in \mathbb{R}^N$, represents the power delivered form generator i, whereas α_i, β_i, and γ_i are cost coefficients of the ith generator. The ED optimization problem then becomes

$$\begin{aligned} &\text{minimize} \quad \sum_i \omega_i C_i(z_i) \\ &\text{s.t.} \quad \sum_i z_i \geq L_d,\ \mathbf{Mz} + \delta \geq 0,\ z_{\min} \leq z_i \leq z_{\max}. \end{aligned} \tag{2}$$

In (2), $\mathbf{M} \in \mathbb{R}^{N\times N}$. ω_i in the objective function is the weighting coefficient, whereas L_d denotes the load demand. The second inequality constraint is generator's power limits between $z_{\min}$ and $z_{\max}$. The third equality constraint in (2) is termed as the consensus constraint. When $\mathbf{Mz} + \delta = 0$, all generators reach at a consensus. By allowing $\delta \geq 0$ and correspondingly $\mathbf{Mz} + \delta \geq 0$, consensus constraint is relaxed, which in turn provides the flexibility to reduce the overall generation cost. To map the constrained optimization problem in (2) to an equivalent unconstrained problem, we use the Lagrange function. The Lagrangian for the optimization problem in (2) is defined as

$$\begin{aligned} L(\mathbf{z}, \lambda, \mathbf{\Phi}, \rho, \sigma) = &\sum_i \omega_i C_i(z_i) + \lambda\left(L_d - \sum_i z_i\right) \\ &+ \Phi^t[\mathbf{Mz} + \delta] + \sum_i \rho(z_{\min} - z_i) \\ &+ \sum_i \sigma(z_i - z_{\max}). \end{aligned} \tag{3}$$

In (3), λ, ρ, σ, and Φ are the Lagrange multipliers (or dual variables) associated with the load demand, consensus constraint, and individual generator's minimum and maximum power limits, respectively. Using (3), next, we construct the primal-dual dynamics, for the optimization problem in (2), given as follows:

$$\begin{aligned} &\dot{z}_i = k_{z_i}(\omega_i C_i'(z_i) + \Phi^t M_i - \lambda - \rho + \sigma) \\ &\dot{\lambda} = k_\lambda\left\{L_d - \sum_i z_i\right\}^+, \quad \dot{\phi}_i = k_{\phi_i}\{[\mathbf{Mz}]_i + \delta\}^+ \\ &\dot{\rho} = k_{\rho_i}\{z_{\min} - z_i\}^+ \quad \dot{\sigma} = k_{\sigma_i}\{z_i - z_{\max}\}^+. \end{aligned} \tag{4}$$

In (4), M_i represents the ith column of $\mathbf{M}$, $[\mathbf{Mz}]_i$ denotes the ith element of vector $\mathbf{Mz}$, and $\phi_i \in \Phi$. The coefficients k_{z_i}, k_λ and k_{ϕ_i}, k_{ρ_i}, k_{σ_i} are controller gains, whereas the notation $\{z\}^+$ in (4) is defined as $\max\{0, z\}$. Let $u_i = \Phi^t M_i - (\lambda + u_\rho - u_\sigma)$ is the control action. Using the expression for λ, ρ, and σ from (4) and substituting to the control action u_i, the system dynamic equations can be rewritten as follows:

$$\begin{aligned} u_i &= \Phi^t M_i - \left(\int_0^t k_\lambda\left(L_d - \sum_i z_i(\tau)\right)^+ d\tau + u_\rho - u_\sigma\right) \\ u_\rho &= \int_0^t k_{\rho_i}(z_{\min} - z_i(\tau))^+ d\tau \\ u_\sigma &= -\int_0^t k_{\sigma_i}(z_i(\tau) - z_{\max})^+ d\tau. \end{aligned} \tag{5}$$

The auxiliary variables consisting of u_i, u_ρ, and u_σ in (5) are in fact part of the control law, which effectively implements an integral control to adjust power generation from each DG.

B. Proposed PID Based ED

Due to the inherent integral control action, the dynamic performance of the optimized power generation may not be satisfactory. To improve the dynamic performance during power transients due to any variations in load demand, a dynamic performance controller based solution is developed. This is achieved by modifying the system dynamics given in (5), to incorporate additional terms. For that purpose, we extend the Lagrangian in (3) to construct an augmented Lagrangian function L_a given by

$$\begin{aligned} L_a(\mathbf{z}, \lambda, \Phi, \rho, \sigma, \tilde{\mathbf{z}}) = &\sum_i \omega_i C_i(z_i) + \sum_i \frac{k_p}{2}\left(L_d - \sum_i z_i\right)^2 \\ &+ k_i\Bigg\{\lambda\left(L_d - \sum_i z_i\right) \\ &+ \Phi^t[\mathbf{Mz} + \delta] + \sum_i \rho(z_{\min} - z_i) \\ &+ \sum_i \sigma(z_i - z_{\max})\Bigg\} + \sum_i \frac{k_d}{2}(z_i - \tilde{z}_i)^2. \end{aligned} \tag{6}$$

In (6) k_p, k_i, and k_d are, respectively, proportional, integral, and derivative gains of the controller and $\tilde{z}_i$ is an auxiliary state variable. Using the augmented Lagrangian in (6), the updated primal-dual dynamics and associated control law u_i becomes

$$\begin{aligned} &\dot{z}_i = k_{z_i}(\omega_i C_i'(z_i) + u_i), \quad \dot{\tilde{z}}_i = \tilde{k}_d(z_i - \tilde{z}_i) \\ &\dot{\lambda} = k_\lambda\left\{L_d - \sum_i z_i\right\}^+, \quad \dot{\phi}_i = k_{\phi_i}\{[\mathbf{Mz}]_i + \delta\}^+ \\ &\dot{\rho} = k_{\rho_i}\{z_{\min} - z_i\}^+, \quad \dot{\sigma} = k_{\sigma_i}\{z_i - z_{\max}\}^+ \\ &u_i = -k_i[\lambda + \rho - \sigma - \Phi^t M_i] \\ &\quad + k_d(z_i - \tilde{z}_i) - k_p\psi(\dot{\lambda}) \quad \forall i. \end{aligned} \tag{7}$$

The first expression in (7) represents the power system dynamics for ED and the associated controller u_i. The control law u_i implements the PID control, where $\psi(.)$ is a linear functional mapping. The first term, in u_i, is the integral control action. The

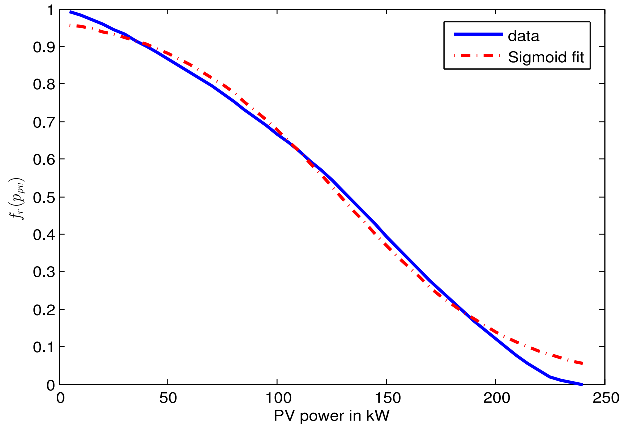

Fig. 3. Sigmoid fit for cumulative distribution function of the PV output power with parameters $a = 0.0259$ and $c = 129$.

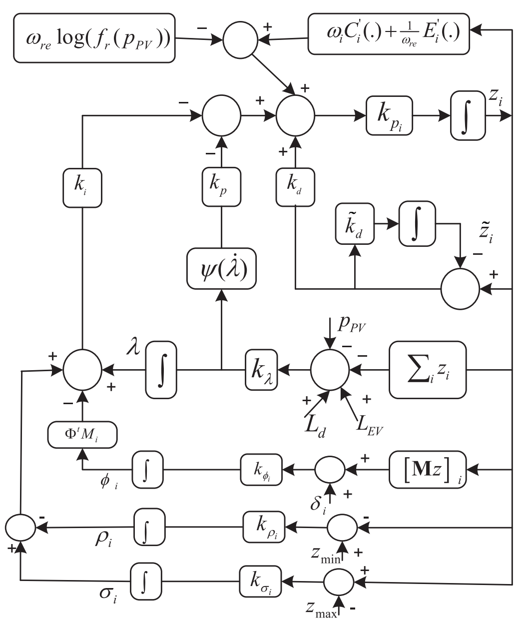

Fig. 4. Block diagram used in MATLAB to simulate PID dynamics.

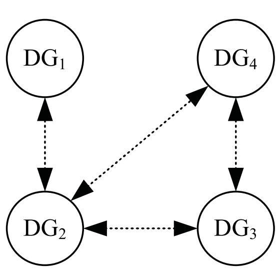

Fig. 5. System configuration of four DGs alongwith a communication structure.

TABLE I
SYSTEM PARAMETERS USED FOR SIMULATION

Parameter	Value
DG1 and DG2 rating	2.0 MVA, 1.5 MVA
DG3 and DG4 rating	1.8 MVA, 2.5 MVA
Load demand	1 MW - 4 MW
Communication rate among DGs	250 kbps

TABLE II
COST COEFFICIENTS FOR DGS

Parameter	DG1	DG2	DG3	DG4
α	$0.01\ 10^{-5}$	1.5×10^{-5}	2.5×10^{-5}	2×10^{-5}
β	5×10^{-3}	2×10^{-3}	2.5×10^{-3}	4×10^{-3}
γ	0.10	0.15	0.09	0.075
a	4.091	2.543	4.258	5.426
b	-5.554	-6.047	-5.094	-3.550
c	6.490	5.638	4.586	3.380

second term is responsible for implementing derivative control action in variable z_i, which can be verified. The second term in u_i, $k_d(z_i - \tilde{z}_i)$, in (7) converges to zero at equilibrium, and equivalently, the auxiliary variable $\tilde{z}_i$ converges to z_i, $\forall i$. This term is responsible for implementing derivative control action in variable z_i, as verified in the following. For this purpose, applying the Laplace transformation to $\dot{\tilde{z}}_i = \tilde{k}_{z_i}(z_i - \tilde{z}_i)$ results in $\tilde{z}_i(s) = \frac{\tilde{k}_{z_i}}{s+\tilde{k}_{z_i}} z_i(s)$. Substituting $\tilde{z}_i(s)$ into the expression $k_d(z_i - \tilde{z}_i)$, it becomes $\frac{k_d}{s+\tilde{k}_{z_i}} s z_i(s)$, which implements derivative control in z_i, whereas the coefficient $\frac{k_d}{s+\tilde{k}_{z_i}}$ implements low-pass filtering. Choosing a large value of gain parameter k_d increases the bandwidth of derivative control. The last term in u_i implements the proportional control action. This can be verified using a simple linear functional mapping as $\psi(\dot{\lambda}) = \dot{\lambda}$. $\dot{\lambda}$ is proportional to z_i and results in proportional control action.

C. *Economic-Emission Dispatch With Renewable Energy Resources*

This section extends the ED problem further by incorporating pollutant emission minimization for CO_2 and integration of PV renewable energy resource. The generated power from PV is stochastic and can be modeled using a probability density function of the PV output power (e.g., see [20, Fig. 3(a)]).

1) Pollutant Emission Cost: Among the three pollutants, NO_x, CO_2, and SO_x, considered in the literature, CO_2 is the most dominant. Pollutant emission cost $E_i(z_i)$ follows quadratic cost [21], [22] and is given by $\sum_i E_i(z_i) = \sum_i a_i z_i^2 + b_i z_i + c_i$, $\forall i$, where a, b, and c are pollutant emission cost coefficients.

2) Reliability Cost for PV Power: The proposed microgrid model incorporates PV energy sources, whose power variation affects the overall power sharing among the DGs of the microgrid. To take into account the intermittency of power from a PV source, we introduce a reliability cost component to the objective function of the optimization problem (9). The operational and maintenance costs of PV are minimal and have been ignored. The reliability objective function $f_r(x)$ is defined as $1 - \Pr(p_{\text{pv}} < x)$, which effectively is a measure of at least obtaining power p_{pv} from the PV source. The term $\Pr(p_{\text{pv}} < x)$ effectively is cumulative distribution function and is obtained from [20] for PV sources. Reader is referred to [20, Fig. 3(b)]. The reliability function is obtained by curve fitting a sigmoid function to the data from [20] and is given by

$$f_r(p_{\text{pv}}) = \frac{e^{-a(p_{\text{pv}}-c)}}{1+e^{-a(p_{\text{pv}}-c)}}. \tag{8}$$

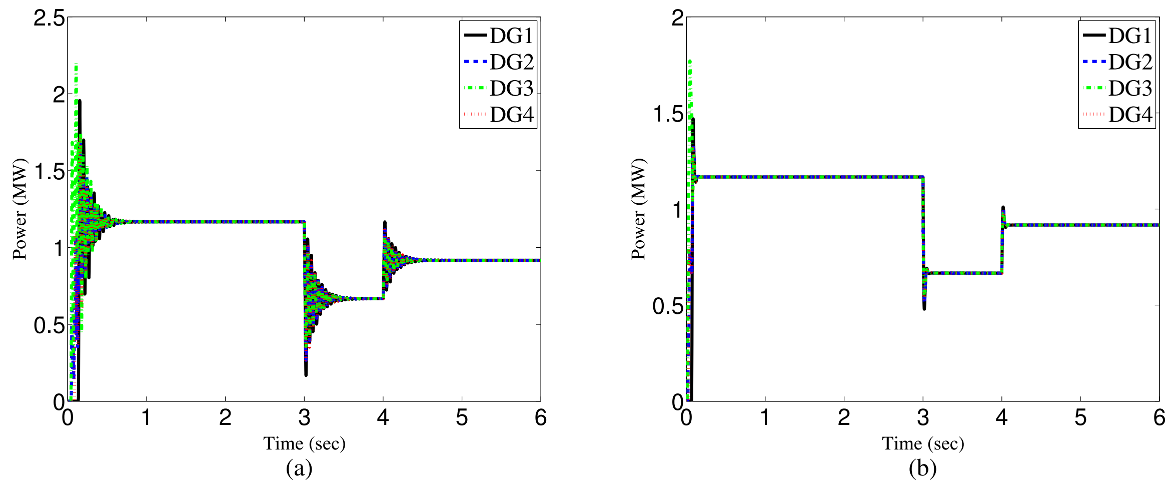

Fig. 6. Consensus among DGs for optimal power generation based on (a) conventional control and (b) PID control.

The result of the sigmoid function fit is shown in Fig. 3. The function $f_r(p_{\text{pv}})$ is nonconvex, however, $\log$ transformation results in a concave function, which is used to maximize the reliability.

3) Optimization Problem Formulation: There is an underlying tradeoff among the conflicting objectives of pollutant emission reduction, PV power reliability enhancement, and generation cost reduction. To achieve this tradeoff, we formulate a weighted multiobjective optimization problem using the weighting coefficients ω_i and ω_{re}, where ω_{re} is the weighting coefficient to provide tradeoff between PV reliability and emissions. The multiobjective ED problem can now be reformulated as follows:

$$\begin{aligned}&\min \sum_i \left\{\omega_i C_i(z_i) + \frac{1}{\omega_{\text{re}}} E_i(z_i)\right\} - \omega_{\text{re}} \log(f_r(p_{\text{pv}}))\\ &\text{s.t.} \sum_i z_i + p_{\text{pv}} = L_d + L_{\text{EV}},\ \sum_i z_i \geq L_d\\ &\mathbf{Mz} + \delta \geq 0,\ \ z_{\min} \leq z_i \leq z_{\max}. \end{aligned} \tag{9}$$

In (9), p_{pv} is the power output from PV panels and L_{EV} is a distributed load due to electric vehicles, which also affects system transients. The problem in (9) can be solved using the Lagrangian duality, as discussed previously.

IV. Performance Evaluation Results

Since this paper is implemented at algorithmic level, most of the results are obtained through numerical simulations of the proposed microgrid system. For that purpose, MATLAB R2016a is used on Intel Core i5 laptop. Please refer to Fig. 4 that has been used for simulating the PID dynamics given in (7) and its extended version given by (9) with their descriptions given in Sections III-B and III-C3, respectively.

For the optimized power flow control from the distributed generation, we consider a network of four DGs [23]. Each DG comprises of a controller module, an energy source, and a power converter. The proposed PID algorithm is applicable for both grid connected as well as islanded mode of operation.

TABLE III
PID Controller Gains

Parameter	DG1	DG2	DG3	DG4
Without Generator Power Limits				
k_p	0.03	0.13	0.07	0.04
k_i	.03	.03	.03	.03
k_d	.2	.36	.4	.12
With Generator Power Limits				
k_p	0.015	0.065	0.035	0.02
k_i	1	1.5	2.5	1.5
k_d	.4	.72	0.8	0.4

The connectivity among the four DGs is illustrated in Fig. 5. For the given connectivity among the DGs, the corresponding Laplacian matrix is given by

$$M = \begin{bmatrix} 1 & -1 & 0 & 0\\ -1 & 3 & -1 & -1\\ 0 & -1 & 2 & -1\\ 0 & -1 & -1 & 2 \end{bmatrix}. \tag{10}$$

The power generation capacities for the four generators are tabulated in Table I. It is assumed that the generators are conventional thermal power units with generator's cost coefficients given in Table II. The generator's cost coefficients in Table II are derived from [24], whereas pollutant emission cost coefficients are taken from [21]. We require a total power demand of 4 MW. The information among the DGs is exchanged using an IEEE 802.15.4-based communication interface, which provides a data rate of 250 Kb/s. The step-size scaling coefficients are configured with constant values as $k_{p_i} = 2000$, $\tilde{k}_{p_i} = 400$, $k_{\phi_i} = 20$, and $k_{\lambda_i} = 30$.

A. Case1: Performance of the Conventional and Proposed PID Controls With Generator Power Constraints

We compare the performance of the optimized PID based ED with that of the conventional ED under generator power constraints and the results are shown in Fig. 6(a) and (b). The

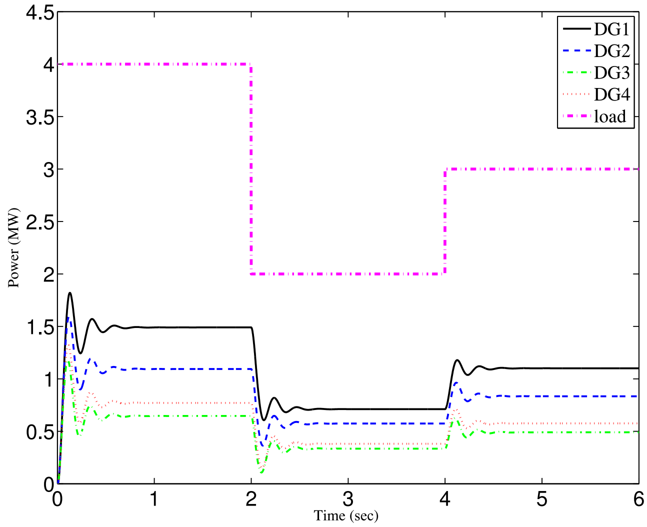

Fig. 7. Optimal power generation from different DGs based on the conventional control.

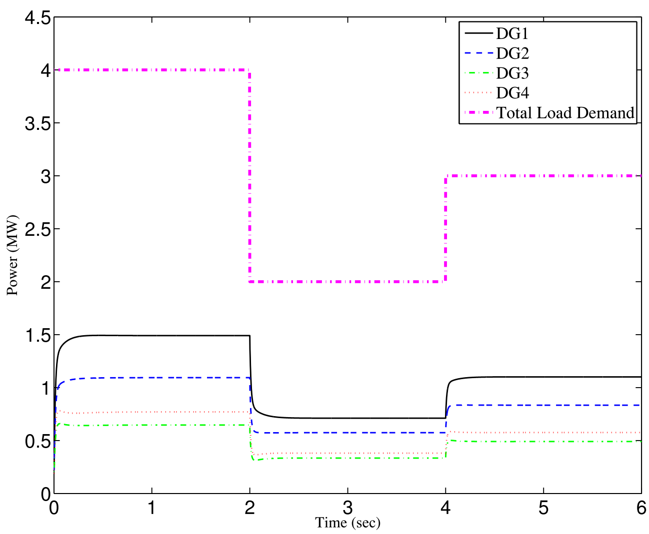

Fig. 8. Optimal power generation from different DGs based on the optimized PID control.

step-size scaling coefficients are configured with constant values as $k_{\rho_i} = 400$, $k_{\phi_i} = 20$, $k_\lambda = 30$, and $k_{\rho_i} = 200$.

Introducing generator's power limits $(z_{\min}, z_{\max})$, conventional control has more pronounced transients compared to PID control. With proper tuning, PID control outperforms the conventional control. The consensus constraint in (2) allows us to achieve any desired tradeoff between cost optimization and uniform loading of multiple DGs. The system also achieves a consensus ensuring that all DGs are generating same power. The tuned values of the PID gains used for this case are tabulated in Table III.

B. Case 2: Performance of PID Without Generator Power Constraints

In this case, we first compare the performance of integrator-based controller with the proposed PID based optimized power generator for ED. In addition, the dynamic performance of the two controllers is also compared. For this scenario, the parameter δ is set equal to one-half of the load demand. This setting restricts the maximum generated power difference between any pair of generators not more than 2 MW. The performance of integral control for ED is shown in Fig. 7. It can be observed from Fig. 7 that system response exhibits poor transient performance. There is high overshoot at the beginning as system tries to adjust the power from different generation units. It takes approximately 0.7 s to reach steady state. At 2 and 4 s, the system experiences a step change in load demands to $\frac{1}{2}L_d$ and $\frac{3}{4}L_d$, respectively, resulting in power transients. For these step changes in the load demand, we observe poor transient performance again. The same load transient scenario is presented to the optimized PID and the response is shown in Fig. 8. The tuned values of the PID gains used for this case are tabulated in Table III. From the results in Fig. 8, we observe a significant improvement in the transient performance and system settles in less than 0.2 s. In addition, the overshoot is also reduced significantly, as can be seen from Fig. 8.

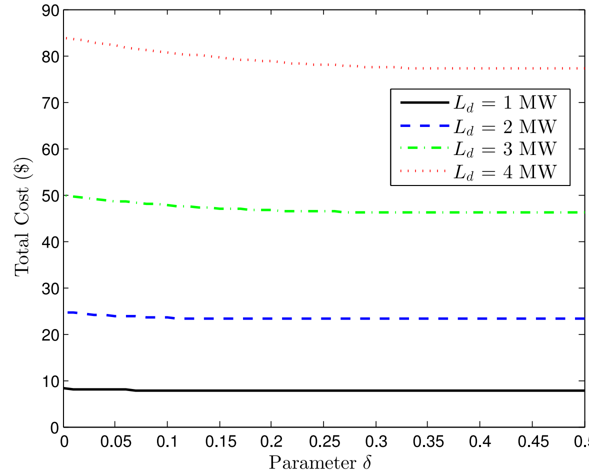

Fig. 9. Effect of parameter δ on total generation cost for different loads.

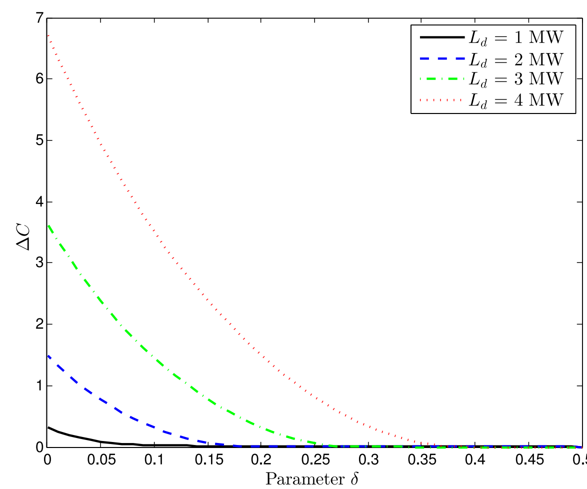

Fig. 10. Incremental generation cost (in \$) as a function of parameter δ for different load demands.

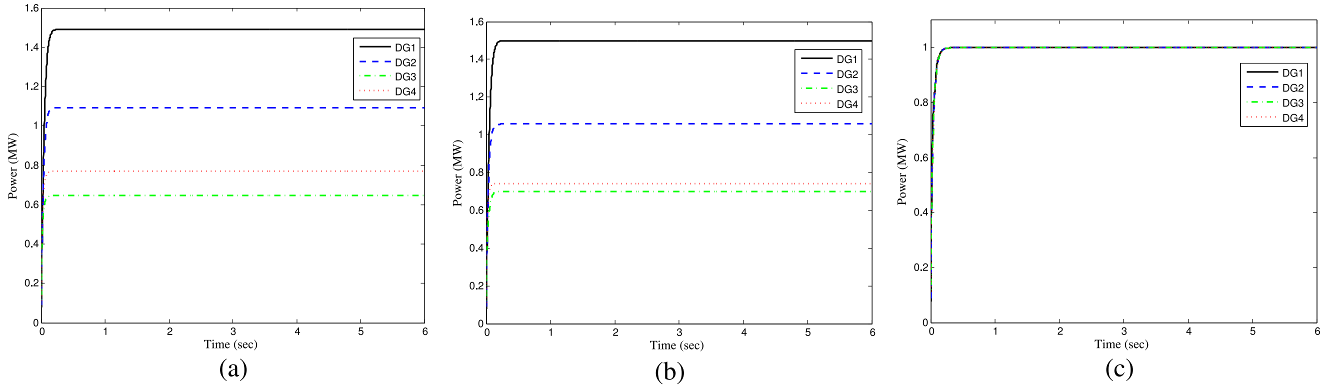

Fig. 11. Effect of δ variations on the power allocation to different DGs. (a) $\delta = 0.8$. (b) $\delta = 0.4$. (c) $\delta = 0$.

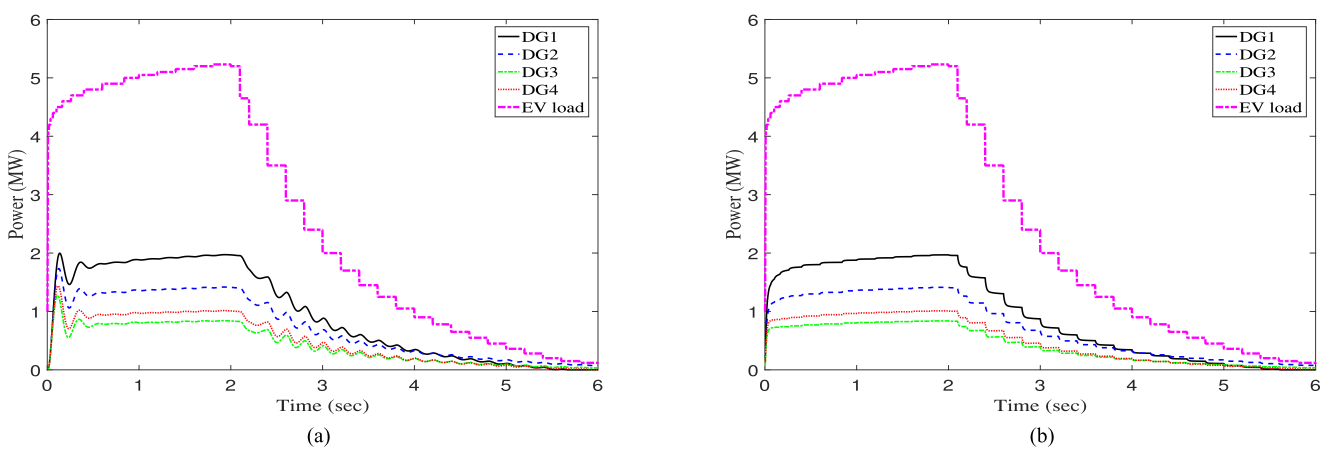

Fig. 12. (a) PI controller performance with EV load. (b) Optimized controller performance with EV load.

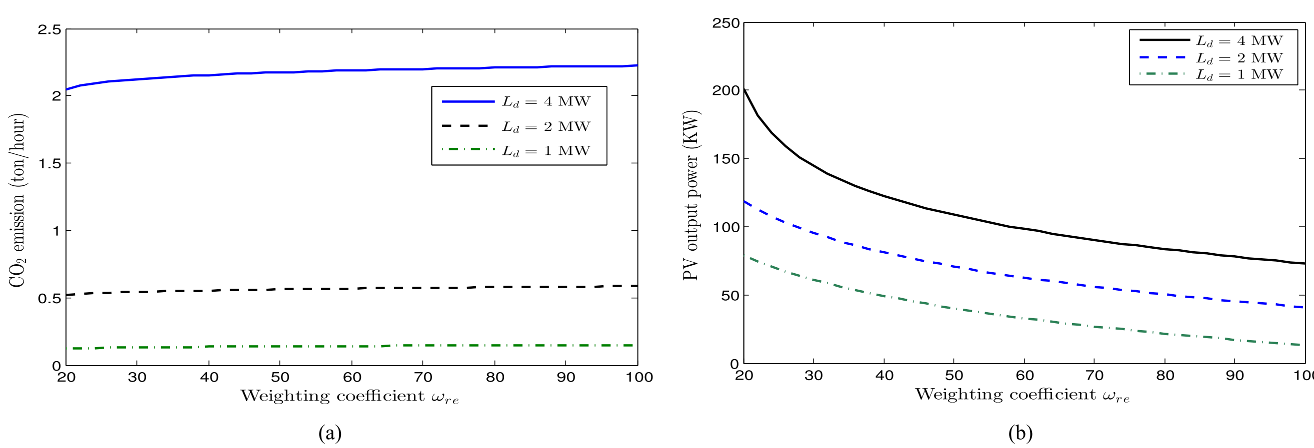

Fig. 13. (a) Effect of pollutant emission. (b) PV power reliability.

C. Case 3: Effect of δ on Generation Cost

Next, we analyze the effect of parameter δ on the total generation cost for different load demands. For a given load demand, increasing δ leads to generation cost reduction, as can be seen from Fig. 9. The cost reduction is based on the fact that a DG with lower cost contributes more power in contrast to a DG with higher generation cost. Increasing δ does not provide cost reduction arbitrarily. Rather, we do not get any cost reduction beyond a certain threshold value of δ, which corresponds to the optimal generation cost and the consensus constraint becomes inactive at that point. For a fixed load demand, let C_δ denote the total generation cost for a given value of δ, whereas $C_{\min}$ denotes the minimum possible generation cost for the same load demand, then we define incremental generation cost, attributed

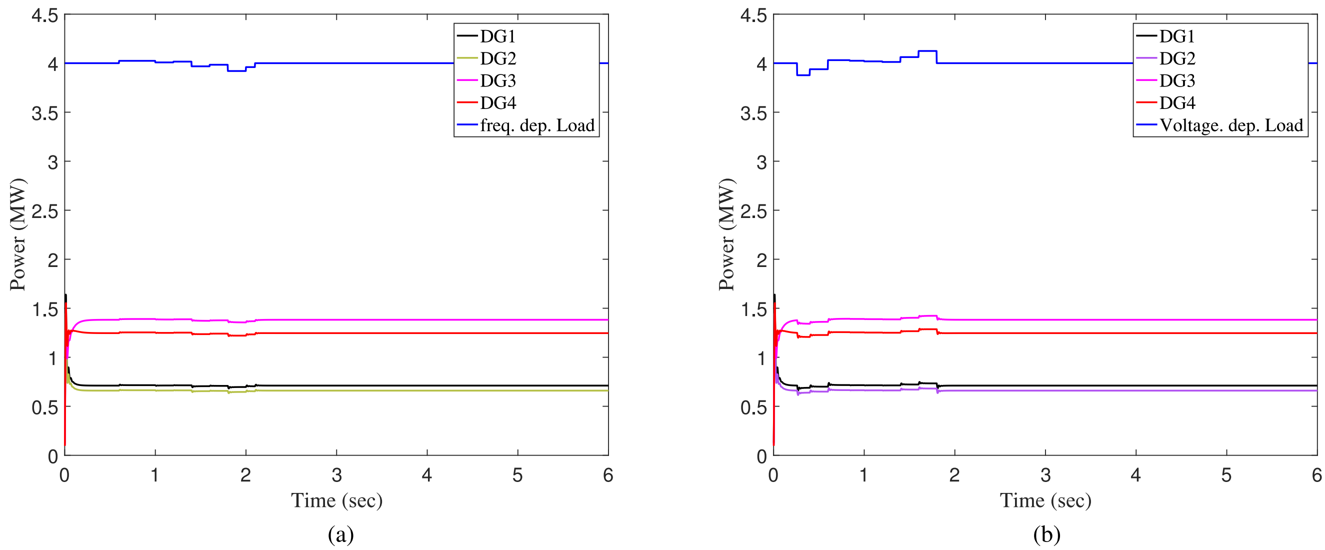

Fig. 14. Impact of (a) frequency-dependent and (b) voltage-dependent loads.

to consensus, as $\Delta C = C_\delta - C_{\min}$. For different load demands, the incremental generation cost ΔC as a function of δ is shown in Fig. 10. As the parameter δ increases, the incremental generation cost reduces and becomes zero beyond the threshold value of δ. The threshold value for δ increases with an increase in the load demand as can be observed from Fig. 10. In addition, an increase in the load demand also results in higher incremental cost, due to the generation from higher cost DGs.

The relaxed consensus constraint in (2) allows to achieve any desired tradeoff between cost optimization and uniform loading of multiple DGs. Setting a large value of parameter δ results in cost optimization, whereas making it zero ensures that all DGs are generating same power. Next, we analyze the effect of varying parameter δ on the power allocation to different DGs. This is shown in Fig. 11 for three different values of parameter δ. Setting a value of 0.8 to parameter δ, the difference between the powers generated from the DGs connected to each other does not exceed 0.8 MW, as can be observed from Fig. 11(a). Similarly, when δ is set to zero, all the DGs are generating same power as verified from Fig. 11(c).

D. Case 4: Effect of Electric Vehicle Load on the Performance of PI and Optimized Controller

To further explore the transient response of the proposed solution, the measured data from [25] is used to construct a load model of EV charging station for a Nissan Leaf EV, having 50-kW charging load. The results are shown in Fig. 12(a) and (b). When the charging load of 5 MW for a fleet of Nissan Leaf EVs is applied for up to 2 s, the generators share this load. Performance of PI control is compared with an optimized controller. As shown in Fig. 12(a), a PI controller has greater transients compared to an optimized controller as shown in Fig. 12(b). After 2 s, the EV load is gradually reduced, the load demand on generators due to EVs is also adjusted and followed closely by the DGs. From these results, it is obvious that an optimized controller has superior dynamic performance compared to a PI controller.

E. Case 5: Effect of Pollutant Emission and PV Power Reliability

Effects of CO_2 emission and PV power reliability are also analyzed using the revised optimization problem in (9) and the results are shown in Fig. 13(a) and (b). Fig. 13(a) shows the increase in CO_2 emissions (ton/hour) as a function of parameter ω_{re} for different loads. In addition, Fig. 13(b) shows the PV power reliability as a function of parameter ω_{re}. From these results, it is obvious that demanding higher reliability reduces PV power contribution to the system.

F. Case 6: Impact of Frequency-Dependent and Voltage-Dependent Loads

Different frequency- and voltage-dependent load models are studied in the literature [26], [27]. Among those ZIP, exponential, and linear frequency dependent models are widely used for load modeling. An exponential load model [28] with both voltage and frequency dependence has been adopted in this study and its impact on transient performance of the microgrid is studied. The load model, used to analyze voltage- and frequency-dependent load variations, is given as follows:

$$L_d(E, w) = P_o \left(\frac{E}{E_o}\right)^{k_{\text{pv}}} \left(1 + k_{pf}\,\frac{w - w_o}{w_o}\right) \tag{11}$$

where $k_{\text{pv}} = 1.7$ and $k_{pf} = 1$ and these are taken from [27] for a residential load. P_o is nominal load that is taken as $4\,$MW, E is system operating voltage, and E_o is nominal voltage. w is the operating frequency and w_o is the nominal frequency. The frequency deviation was taken from -1% to 0.6% and its effect is shown in Fig. 14(a) for frequency-dependent load. The voltage deviation was taken from -2% to 2% and the corresponding result is shown in Fig. 14(b). The accumulated power from DGs follows closely the required voltage-dependent and frequency-dependent load power, as observed from these results.

V. Conclusion

The problem of the optimized control for ED in microgrid-based distributed generation is considered. To overcome the performance limitations of integral-based control, PID-based optimized control is proposed that provides an improved dynamic performance. In particular, the augmented Lagrangian approach is used to design the dynamic controller providing a tight control of system dynamics. In addition, a consensus constraint is introduced to tradeoff between cost optimality and power sharing among DGs. The PID performance is compared with the conventional integral based control for ED in a microgrid. Furthermore, electric vehicle type load is included in system to further study load intermittency. Impact of frequency-dependent and voltage-dependent loads are also analyzed.

The proposed solution can be extended for event-driven ED, in the multiagent framework, to further reduce the communication bandwidth requirements. An optimization formulation can also be investigated for a multimicrogrid case with energy routing to meet energy internet requirements.

References

[1] F. Katiraei and M. R. Iravani, “Power management strategies for a microgrid with multiple distributed generation units,” *IEEE Trans. Power Syst.*, vol. 21, no. 4, pp. 1821–1831, Nov. 2006.

[2] M. Jain, S. Gupta, D. Masand, and G. Agnihotri, “Analysis of a microgrid under transient conditions using voltage and frequency controller,” *Adv. Power Electron.*, vol. 2012, 2012. [Online]. Available: https://www.hindawi.com/journals/ape/2012/208231/

[3] M. L. Fisher, “The Lagrangian relaxation method for solving integer programming problems,” *Manage. Sci.*, vol. 50, no. 12, pp. 1861–1871, 2004. [Online]. Available: http://www.jstor.org/stable/30046157

[4] C.-L. Chen and N. Chen, “Direct search method for solving economic dispatch problem considering transmission capacity constraints,” *IEEE Trans. Power Syst.*, vol. 16, no. 4, pp. 764–769, Nov. 2001.

[5] A. G. Tsikalakis and N. D. Hatziargyriou, “Centralized control for optimizing microgrids operation,” in *Proc. IEEE Power Energy Soc. Gen. Meeting*, Jul. 2011, pp. 1–8.

[6] A. Cherukuri and J. Corts, “Distributed generator coordination for initialization and anytime optimization in economic dispatch,” *IEEE Trans. Control Netw. Syst.*, vol. 2, no. 3, pp. 226–237, Sep. 2015.

[7] Y. Xu and Z. Li, “Distributed optimal resource management based on the consensus algorithm in a microgrid,” *IEEE Trans. Ind. Electron.*, vol. 62, no. 4, pp. 2584–2592, Apr. 2015.

[8] W. T. Elsayed and E. F. El-Saadany, “A fully decentralized approach for solving the economic dispatch problem,” *IEEE Trans. Power Syst.*, vol. 30, no. 4, pp. 2179–2189, Jul. 2015.

[9] V. Loia and A. Vaccaro, “Decentralized economic dispatch in smart grids by self-organizing dynamic agents,” *IEEE Trans. Syst. Man, Cybern., Syst.*, vol. 44, no. 4, pp. 397–408, Apr. 2014.

[10] F. Chen *et al.*, “Cost-based droop schemes for economic dispatch in islanded microgrids,” *IEEE Trans. Smart Grid*, vol. 8, no. 1, pp. 63–74, Jan. 2017.

[11] W. Hu, P. Wang, and H. B. Gooi, “Toward optimal energy management of microgrids via robust two-stage optimization,” *IEEE Trans. Smart Grid*, vol. 9, no. 2, pp. 1161–1174, Mar. 2018.

[12] Y. Zhang, M. H. Hajiesmaili, S. Cai, M. Chen, and Q. Zhu, “Peak-aware online economic dispatching for microgrids,” *IEEE Trans. Smart Grid*, vol. 9, no. 1, pp. 323–335, Jan. 2018.

[13] J. Zhao and P. L, “Decentralized two-stage control for active power real time dispatch in islanded ac microgrids,” in *Proc. IEEE Conf. Energy Internet Energy Syst. Integr.*, Nov. 2017, pp. 1–6.

[14] Y. A. Abass, A. T. Al-Awami, and T. Jamal, “Integrating automatic generation control and economic dispatch for microgrid real-time optimization,” in *Proc. IEEE Power Energy Soc. Gen. Meeting*, 2016, pp. 1–5.

[15] N. Cai, N. T. T. Nga, and J. Mitra, “Economic dispatch in microgrids using multi-agent system,” in *Proc. North Amer. Power Symp.*, 2012, pp. 1–5.

[16] J. M. Guerrero, J. C. Vasquez, J. Matas, L. G. de Vicuña, and M. Castilla, “Hierarchical control of droop-controlled ac and dc microgrids general approach toward standardization,” *IEEE Trans. Ind. Electron.*, vol. 58, no. 1, pp. 158–172, Jan. 2011.

[17] A. Bidram, A. Davoudi, F. L. Lewis, and Z. Qu, “Secondary control of microgrids based on distributed cooperative control of multi-agent systems,” *IET Gener. Transmiss. Distrib.*, vol. 7, no. 8, pp. 822–831, Aug. 2013.

[18] N. M. Dehkordi, N. Sadati, and M. Hamzeh, “Fully distributed cooperative secondary frequency and voltage control of islanded microgrids,” *IEEE Trans. Energy Convers.*, vol. 32, no. 2, pp. 675–685, Jun. 2017.

[19] A. Bidram and A. Davoudi, “Hierarchical structure of microgrids control system,” *IEEE Trans. Smart Grid*, vol. 3, no. 4, pp. 1963–1976, Dec. 2012.

[20] G. Tina, S. Gagliano, and S. Raiti, “Hybrid solar/wind power system probabilistic modelling for long-term performance assessment,” *Sol. Energy*, vol. 80, no. 5, pp. 578–588, 2006.

[21] A. Jubril, O. Olaniyan, O. Komolafe, and P. Ogunbona, “Economic-emission dispatch problem: A semi-definite programming approach,” *Appl. Energy*, vol. 134, no. Suppl. C, pp. 446–455, 2014.

[22] H. Kanchev, F. Colas, V. Lazarov, and B. Francois, “Emission reduction and economical optimization of an urban microgrid operation including dispatched PV-based active generators,” *IEEE Trans. Sustain. Energy*, vol. 5, no. 4, pp. 1397–1405, Oct. 2014.

[23] M. Tahir and S. K. Mazumder, “Self-triggered communication enabled control of distributed generation in microgrids,” *IEEE Trans. Ind. Inform.*, vol. 11, no. 2, pp. 441–449, Apr. 2015.

[24] Y. Xu, W. Zhang, and W. Liu, “Distributed dynamic programming-based approach for economic dispatch in smart grids,” *IEEE Trans. Ind. Inform.*, vol. 11, no. 1, pp. 166–175, Feb. 2015.

[25] R. C. Leou, J. H. Teng, and C. L. Su, “Modelling and verifying the load behaviour of electric vehicle charging stations based on field measurements,” *IET Gener. Transmiss. Distrib.*, vol. 9, no. 11, pp. 1112–1119, 2015.

[26] S. Palm and P. Schegner, “Static and transient load models taking account voltage and frequency dependence,” in *Proc. Power Syst. Comput. Conf.*, Jun. 2016, pp. 1–7.

[27] I. T. F. on Load Representation for Dynamic Performance, “Load representation for dynamic performance analysis [of power systems],” *IEEE Trans. Power Syst.*, vol. 8, no. 2, pp. 472–482, May 1993.

[28] H. H. Zeineldin and J. L. Kirtley, “Micro-grid operation of inverter based distributed generation with voltage and frequency dependent loads,” in *Proc. IEEE Power Energy Soc. Gen. Meeting*, Jul. 2009, pp. 1–6.

Jameel Ahmad received the B.Sc. degree in electrical engineering from the University of Engineering and Technology (UET) Peshawar, Peshawar, Pakistan, in 1993, and the M.Sc. degree in electrical engineering from the University of Southern California at Los Angeles, Los Angeles, CA, USA, in 2005. He is currently working toward the Ph.D. degree in electrical engineering at the Department of Electrical Engineering, UET Lahore, Lahore, Pakistan, under the supervision of Dr. M. Tahir.

He was with Qualcomm and Broadcom Corporation, San Diego, CA, USA, from June 2007 to June 2010, on 2G and 3G mobile communication systems. Since August 2010, he has been an Assistant Professor with the Department of Electrical Engineering, School of Engineering, University of Management and Technology Lahore, Lahore, Pakistan. His research interests include control and optimization of smart microgrids for energy internet.

Prof. Ahmad is the reviewer of numerous IEEE journals and conferences.

Muhammad Tahir (M'02) received the Ph.D. degree in electrical and computer engineering from the University of Illinois at Chicago, Chicago, IL, USA, in 2008.

He is currently an Associate Professor with the Department of Electrical Engineering, University of Engineering and Technology Lahore, Lahore, Pakistan. He was a Visiting Research Scholar with the University of Illinois at Chicago in the summer of 2014. He was the principal investigator on the funded research projects related to air quality monitoring and intelligent camera networks. He has more than 40 international publications to his credit. His research interests include wireless sensor networks, delay-tolerant networks, distributed resource optimization for wireless networks, and real-time wireless multimedia networks.

Dr. Tahir is the reviewer of numerous IEEE journals and conferences.

Sudip K. Mazumder (S'97–M'01–SM'03–F'16) received the Ph.D. degree in electrical and computer engineering from Virginia Tech, Blacksburg, VA, USA, in 2001.

He has been a Professor with the University of Illinois at Chicago (UIC), Chicago, IL, USA, since 2001, and has been the President of NextWatt LLC since 2008. He has more than 25 years of professional experience and has held R&D and design positions in leading industrial organizations and has served as a Technical Consultant for several industries. He has authored or coauthored more than 200 refereed papers, delivered more than 85 keynote/plenary/invited presentations, and received and carried out about 50 sponsored research projects since joining UIC. He is the author or co-author of more than 180 journal and conference papers and 9 book/book chapters, and holds 8 issued and several pending patents.

Dr. Mazumder was the Guest Editor-in-Chief and an Associate Editor for multiple IEEE Transactions and the first Editor-in-Chief for *Advances in Power Electronics*. He has served and is serving in high-profile capacities in leading IEEE conferences, technical committees, and NSF panels. He was the recipient of several prestigious awards including the UIC's Inventor of the Year Award (2014), the University of Illinois' University Scholar Award (2013), the IEEE PELS Transaction Prize Paper Award (2001), the IEEE Future Energy Challenge Award (2005), the ONR Young Investigator Award (2005), and the NSF CAREER Award (2003).